Functional renormalization group and quantum tunnelling

2006 J. Phys. A: Math. Gen. 39 649

(http://iopscience.iop.org/0305-4470/39/3/015)

INSTITUTE OF PHYSICS PUBLISHING JOURNAL OF PHYSICS A: MATHEMATICAL AND GENERAL

J. Phys. A: Math. Gen. **39** (2006) 649–666 doi:10.1088/0305-4470/39/3/015

Functional renormalization group and quantum tunnelling

Michael Weyrauch

Physikalisch–Technische Bundesanstalt, D-38116 Braunschweig, Germany

E-mail: michael.weyrauch@ptb.de

Received 27 June 2005, in final form 10 November 2005
Published 21 December 2005
Online at stacks.iop.org/JPhysA/39/649

Abstract
A functional renormalization group approach is applied to a single quantum particle with emphasis on quantum tunnelling through a barrier. We include both an effective potential and a wavefunction renormalization and compare the effects of soft cut-off, hard cut-off and Schwinger proper time regulators. Numerical procedures and results are studied in detail.

PACS numbers: 03.65.−w, 03.65.Db, 03.65.Xp, 11.10.Gh

1. Introduction

A detailed study of quantum tunnelling requires non-perturbative methods. The double-well potential provides a good example: the energy gap between ground state and first excited state becomes exponentially small in a nonanalytic way, $\Delta E \sim \exp(-1/g)$, where g is the quartic coupling, and standard perturbative methods fail. In Langer's analysis of the double-well potential in terms of instantons [1] the exponentially small energy gap for large barriers is obtained but the approach fails for small barriers. The instanton approach corresponds to a path integral calculation of the free energy and includes fluctuations around the minimum of the action up to quadratic order.

The renormalization group provides a method of calculating path integrals non-perturbatively. Wilson invented this method in order to study phase transitions and critical phenomena. A detailed account of this development is given in [2]. In section 11 of this reference, a differential form of the renormalization group equation was proposed, which was called *exact* renormalization group equation. This equation takes the form of a functional differential equation and is difficult to solve.

Subsequently, various renormalization group equations in differential form have been studied, e.g. the Wegner–Houghton equation [3] or the Polchinski equation [4]. Wetterich [5] and Morris [6] proposed the exact functional renormalization group equation for the effective action. All these renormalization group equations are closely related and an interesting overview of the various forms is presented in [7].

It was only relatively recently that the functional renormalization group approach was applied to the study of tunnelling in zero-dimensional (0D) systems. In 1998, Aoki *et al* [8] studied the Wegner–Houghton equation for the effective potential and calculated explicitly ground and excited state energies of anharmonic oscillators and double-well potentials. Similar calculations, also based on the Wegner–Houghton equation, but using different numerics, have been presented in [9] and [10]. More recently, Hedden *et al* [11] studied anharmonic oscillators as well as a single Kondo impurity using a functional renormalization group approach with a sharp cut-off. The relation between their approach and the effective potential used in other works is clarified in [12].

In the present paper, we want to study tunnelling in 0D systems starting from the exact renormalization group equation for the effective action as proposed in [5] and [6]. We will compare various renormalization group equations for the effective potential and will also include a wavefunction renormalization. We will address numerical issues, and compare results with high precision calculations using standard operator techniques.

The renormalization flow of the effective average action $\Gamma_k[\phi]$ is given by (see e.g. [5])

$$\frac{\partial}{\partial k}\Gamma_k[\phi] = \frac{1}{2}\,\mathrm{Tr}\big(\Gamma_k^{(2)}[\phi] + R_k\big)^{-1}\frac{\partial}{\partial k}R_k. \tag{1}$$

Here, $\Gamma_k^{(2)}[\phi]$ represents the second functional derivative of $\Gamma_k[\phi]$ with respect to ϕ and corresponds to the inverse single particle propagator. It depends on the classical field ϕ, which in a Landau–Ginzburg type theory is known as the 'order parameter'. The regulator R_k vanishes for $k = 0$, i.e. at $k = 0$ all quantum fluctuations are included in the calculation, while for $k > 0$ quantum fluctuations below a certain limit are suppressed or even excluded. If R_k completely excludes quantum fluctuations below some limit, R_k is called a hard cut-off. Otherwise, R_k will be called a soft cut-off function. The Tr symbol indicates a trace over all quantum numbers labelling the classical field ϕ. Equation (1) represents a functional differential equation, and it is via suitable truncations that this equation is transformed into more tractable partial differential equations. If we can solve the flow equation, then from $\Gamma_0[\phi]$, which represents the Legendre transform of the partition function $Z[J]$, all physical quantities of interest may be obtained, e.g. ground and excited state energies.

Of course, in order to solve the flow equation (1) one needs suitable initial conditions. If we require the regulator to dominate all other quantities at $k = \Lambda$, one can straightforwardly prove [13] that the effective average action takes the form

$$\Gamma_\Lambda[\phi] = C_\Lambda + S[\phi] \tag{2}$$

at $k = \Lambda$, where $S[\phi]$ is the classical action which itself is essentially determined by the classical potential $V(\phi)$ in which the quantum particle moves. The constant C_Λ depends on the choice of the regulator and will be determined for specific regulators in the following section.

There is another functional renormalization group equation for Γ_k which has received some attention in the literature [14, 15]:

$$\frac{\partial}{\partial k}\Gamma_k[\phi] = -\frac{1}{2}\int_0^\infty \frac{\mathrm{d}s}{s}\left(\frac{\partial f_k(s)}{\partial k}\right)\mathrm{Tr}\,\exp\left\{-s\Gamma_k^{(2)}[\phi]\right\}. \tag{3}$$

This is the Schwinger proper time renormalization group equation (PTRG). In fact, the most detailed analysis for 0D systems has been made using this equation [15]. Therefore, we include it here for comparison. A rigorous derivation of equation (3) is not available, however, plausibility arguments are presented e.g. in [7]. Here, f_k is the regulator, which must be chosen appropriately. For details we refer to [14, 15].

The effective action $\Gamma_0[\phi]$ as a functional of ϕ is convex. For a double-well potential, the effective average action $\Gamma_k[\phi]$ remains non-convex during the main part of the flow and becomes convex only close to the endpoint of the renormalization flow at $k = 0$. In fact, one finds that the effective potential, which is closely related to the effective average action, is nearly flat, but not constant, between the two wells. Beyond the minima of the wells the effective potential becomes very steep. In this way, it is possible for the energy gap between ground and excited states to become exponentially small. The correct description of these features poses a significant challenge for the numerical procedure that is used to solve the renormalization group equations.

In section 2, we will discuss truncations of the above two functional renormalization group equations, which reduce them to a set of coupled partial differential equations. This is a formal but very critical step, since it is somewhat uncontrolled. However, in our context we are able to assess the validity of the truncation because we can compare our results to standard calculations using operator techniques. Equations for the effective potential U_k coupled to the wavefunction renormalization Z_k will be derived. In section 3, two methods will be discussed to solve these sets of coupled partial differential equations numerically. Results for various zero-dimensional systems will be analysed in detail.

2. Truncations

In order to solve the functional differential equation (1) a suitable approximation or truncation must be introduced. To this end, we assume that the effective average action takes a specific form, e.g.

$$\Gamma_k[\phi] = \int_0^\beta \mathrm{d}\tau \frac{1}{2}\left(\frac{\mathrm{d}\phi(\tau)}{\mathrm{d}\tau}\right)^2 + U_k(\phi(\tau)). \tag{4}$$

The quantity $U_k(\phi)$ is called the 'effective potential' and $\beta = 1/T$ is the inverse temperature. In the present paper, we consider zero temperature only, i.e. $\beta = \infty$.

More often than not the classical equations of motion are solved by a constant field ϕ_0. This field, however, does not necessarily minimize the action, but may be a maximum (or saddle point in higher dimensions) as is the case for the double-well potential. We first expand the effective potential $U_k(\phi(\tau))$ around this constant field ϕ_0 [$\phi(\tau) = \phi_0 + \psi(\tau)$],

$$U_k(\phi) = U_k(\phi_0) + U_k'(\phi_0)\psi(\tau) + \tfrac{1}{2}U_k''(\phi_0)\psi^2(\tau) + \cdots, \tag{5}$$

where the primes denote derivatives with respect to ϕ_0. Correspondingly, we obtain an expansion of the inverse propagator

$$\Gamma_k^{(2)}[\phi] = \left[U_k''(\phi_0) - \partial_\tau^2\right]\delta(\tau - \tau'). \tag{6}$$

Inserting this result into equation (1), evaluating the trace in Fourier space, and comparing coefficients on both sides of equation (1) we obtain the following flow equation for the effective potential:

$$\frac{\partial}{\partial k}U_k(\phi_0) = \frac{1}{2}\int_{-\infty}^{\infty}\frac{\mathrm{d}\omega}{2\pi}\frac{\partial_k R_k}{U_k''(\phi_0) + \omega^2 + R_k}. \tag{7}$$

This flow equation for the effective potential is a nonlinear partial differential equation depending on two variables, k and ϕ_0.

For practical calculations a suitable regulator must be chosen. In general, we distinguish between soft and hard cut-off regulator functions. For a given k, a hard cut-off excludes fluctuations with low frequencies completely from the integration in the corresponding functional integral, while a soft cut-off only suppresses such low frequency fluctuations.

Furthermore, a suitable regulator must dominate all other quantities involved in the renormalization flow for large k. Suitable choices for a smooth cut-off are e.g. power laws in k. To be specific, we choose $R_k = k^2$, which proves to be a good choice as will be discussed later. The ω-integral may be performed easily and one finds

$$\frac{\partial}{\partial k} U_k(\phi_0) = \frac{1}{2}\left(1 + \frac{1}{k^2} U_k''(\phi_0)\right)^{-\frac{1}{2}}. \tag{8}$$

The initial condition for this equation is given by $U_{k=\Lambda}(\phi_0) = \frac{1}{2}\Lambda + V(\phi_0)$. The large constant $\frac{1}{2}\Lambda$ may be obtained as follows: if we neglect U_k'' in equation (8) we have a flow equation for the regulator itself, $\partial_k U_k = \frac{1}{2}$. Choosing the zero point of the energy scale by setting $U_0 = 0$ one finds $U_k = \frac{1}{2}k$.

A suitable hard cut-off is given by $R_k(\omega) = Nk^2\theta(k^2 - \omega^2)$ with N a large constant. Performing the ω-integration one obtains the Wegner–Houghton equation [3, 16]

$$\frac{\partial}{\partial k} U_k(\phi_0) = -\frac{1}{2\pi} \ln\left(1 + \frac{1}{k^2} U_k''(\phi_0)\right), \tag{9}$$

where an irrelevant large constant has been omitted. This is reflected in the initial condition used for the Wegner–Houghton equation $U_\Lambda(\phi_0) = V(\phi_0)$. Finally, for the PTRG equation one obtains

$$\frac{\partial}{\partial k} U_k(\phi_0) = \frac{1}{\sqrt{4\pi}} \exp\left(-\frac{1}{k^2} U_k''(\phi_0)\right) \tag{10}$$

using a regulator as described in detail in [14, 15]. For this equation the initial condition is given by $U_\Lambda(\phi_0) = \Lambda/\sqrt{4\pi} + V(\phi_0)$.

While the renormalization flow of the various equations is different due to the different regulators, the physical results obtained at $k = 0$ should not depend on the choice of the regulator. This will be investigated in some detail in the following section. It is an instructive exercise to show that all equations yield the correct and exact ground and excited state energy for the harmonic oscillator.

A more advanced truncation of the renormalization group equation also includes a wavefunction renormalization. Then the effective average action is expressed as

$$\Gamma_k[\phi] = \int_0^\infty \mathrm{d}\tau \frac{1}{2} Z_k(\phi(\tau)) \left(\frac{\mathrm{d}\phi(\tau)}{\mathrm{d}\tau}\right)^2 + U_k(\phi(\tau)). \tag{11}$$

The function $Z_k(\phi(\tau))$ is called the 'wavefunction renormalization'. We now expand both $Z_k(\phi)$ and $U_k(\phi)$ around the constant field ϕ_0 [$\phi(\tau) = \phi_0 + \psi(\tau)$]. In order to calculate the inverse propagator we now need an expansion of $\Gamma_k[\phi]$ up to fourth order in the fluctuation field ψ around the constant field ϕ_0. Hence, the second-order functional derivative of Γ_k is given by

$$\begin{aligned}
\Gamma_k^{(2)}[\phi] = {} & \left[U_k'' - Z_k\partial_\tau^2\right]\delta(\tau - \tau') + \Bigg[\frac{1}{2}U_k^{(4)}\psi^2(\tau) + U_k'''\psi(\tau) - Z_k'\psi(\tau)\partial_\tau^2 \\
& - Z_k'\frac{\mathrm{d}\psi(\tau)}{\mathrm{d}\tau}\partial_\tau - Z_k'\frac{\mathrm{d}^2\psi(\tau)}{\mathrm{d}\tau^2} - \frac{1}{2}Z_k''\left(\frac{\mathrm{d}\psi(\tau)}{\mathrm{d}\tau}\right)^2 \\
& - Z_k''\psi(\tau)\frac{\mathrm{d}\psi(\tau)}{\mathrm{d}\tau}\partial_\tau - Z_k''\psi(\tau)\frac{\mathrm{d}^2\psi(\tau)}{\mathrm{d}\tau^2} - \frac{1}{2}Z_k''\psi^2(\tau)\partial_\tau^2\Bigg]\delta(\tau - \tau') \\
= {} & [A_0(\tau) + A_1(\tau)]\delta(\tau - \tau').
\end{aligned} \tag{12}$$

where A_0 does not depend on the fluctuations ψ, while A_1 contains terms dependent on the fluctuation field ψ and its derivatives. We need to obtain the derivative expansion of the inverse of this operator plus R_k. This is accomplished as follows: first we define

$$Q(\tau) = \mathrm{e}^{-\mathrm{i}\omega\tau}(A_0(\tau) + A_1(\tau) + R_k)^{-1}\,\mathrm{e}^{\mathrm{i}\omega\tau} \tag{13}$$

and show that $Q(\tau)$ fulfils the following equation,

$$Q(\tau) = \mathrm{e}^{-\mathrm{i}\tau\omega}\frac{1}{A_0(\tau)+R_k}\,\mathrm{e}^{\mathrm{i}\tau\omega} - \mathrm{e}^{-\mathrm{i}\tau\omega}\frac{1}{A_0(\tau)+R_k}A_1(\tau)\,\mathrm{e}^{\mathrm{i}\tau\omega}Q(\tau), \tag{14}$$

which may be used to calculate $Q(\tau)$ iteratively. Each iteration contains higher orders of A_1 and, therefore, higher order terms in ψ and its derivatives. We obtain up to second order in A_1

$$Q(\tau) = \mathrm{e}^{-\mathrm{i}\tau\omega}\left(\frac{1}{B} - \frac{1}{B}A_1\frac{1}{B} + \frac{1}{B}A_1\frac{1}{B}A_1\frac{1}{B}\right)\mathrm{e}^{\mathrm{i}\tau\omega} + \cdots \tag{15}$$

with $B = A_0 + R_k$. Finally, we move the innermost $1/B$ in the last term to the left using a formula given in the appendix and obtain

$$\begin{aligned} Q(\tau) = \mathrm{e}^{-\mathrm{i}\tau\omega}\Bigg(&\frac{1}{B} - \frac{1}{B}A_1\frac{1}{B} + \frac{1}{B^2}A_1^2\frac{1}{B} + \frac{1}{B^3}[B, A_1]A_1\frac{1}{B} \\ &+ \frac{1}{B^4}[B,[B,A_1]]A_1\frac{1}{B}\Bigg)\mathrm{e}^{\mathrm{i}\tau\omega} + \cdots. \end{aligned} \tag{16}$$

Now it is easy to operate with $1/B$ on the exponentials and to calculate the trace in equation (1) in the Fourier space. Comparing coefficients on both sides of equation (1) one obtains two coupled flow equations for the effective potential U_k and for the wavefunction renormalization Z_k.

After some straightforward but lengthy algebra, which is best performed by a computer program for symbolic computation, we obtain

$$\begin{aligned} \frac{\partial}{\partial k}U_k &= \frac{1}{2\sqrt{Z_k}}\left(1+\frac{U_k''}{k^2}\right)^{-\frac{1}{2}}, \\ \frac{\partial}{\partial k}Z_k &= \frac{1}{2\sqrt{Z_k}}\left(1+\frac{U_k''}{k^2}\right)^{-\frac{1}{2}} \\ &\quad\times\left(-\frac{1}{2}\frac{Z_k''}{U_k''+k^2} + \frac{7}{16}\frac{(Z_k')^2}{Z_k(U_k''+k^2)} + \frac{9}{8}\frac{Z_k'U_k'''}{(U_k''+k^2)^2} - \frac{5}{16}\frac{Z_k(U_k''')^2}{(U_k''+k^2)^3}\right) \end{aligned} \tag{17}$$

for the soft cut-off $R_k = k^2$.

For the hard cut-off $R_k(\omega) = Nk^2\theta(k^2-\omega^2)$ with N a large constant, we obtain

$$\begin{aligned} \frac{\partial}{\partial k}U_k &= -\frac{1}{2\pi}\ln\left(\frac{A_k}{k^2}\right), \\ \frac{\partial}{\partial k}Z_k &= \frac{1}{2\pi}\left(\frac{Z_k''}{A_k} - 2\frac{Z_k'A_k'}{A_k^2} - \frac{(kZ_k')^2}{A_k^2} + \frac{10}{3}\frac{k^4Z_k(Z_k')^2}{A_k^3}\right. \\ &\quad\left. + 4\frac{k^2Z_kZ_k'U_k'''}{A_k^3} + \frac{2}{3}\frac{Z_k(U_k''')^2}{A_k^3} - 2\frac{k^2Z_k^2(A_k')^2}{A_k^4}\right) \end{aligned} \tag{18}$$

defining $A_k = k^2Z_k + U_k''$. For a four-dimensional theory an analogous result has been obtained in [17].

Finally, we consider the corresponding equations for the PTRG. They have been studied before in [15] but without giving details of the derivation. According to equation (3), we need

to calculate the integral

$$-\frac{1}{2}\int_0^\infty \frac{\mathrm{d}s}{s}\left(\frac{\partial f_k(s)}{\partial k}\right)\mathrm{Tr}\,\exp\left(-s\Gamma_k^{(2)}\right) = -\frac{1}{2}\int_0^\infty \frac{\mathrm{d}s}{s}\left(\frac{\partial f_k(s)}{\partial k}\right)\int \mathrm{d}\tau\,\langle\tau|\mathrm{e}^{-s(A_0+A_1)}|\tau\rangle. \tag{19}$$

Here, we insert equation (12) for $\Gamma_k^{(2)}$ and use f_k as given in [15]. This formula corresponds to equation (5) in [14]. In order to disentangle the exponential one needs the Zassenhaus formula [18]. Details are given in the appendix. If one inserts equation (A.7) from the appendix into equation (19) above and transforms into the Fourier space, one obtains after some algebra two coupled equations for U_k and Z_k:

$$\begin{aligned}\frac{\partial U_k}{\partial k} &= \frac{1}{\sqrt{4\pi}}\exp\left(-\frac{U_k''}{Z_k k^2}\right)\\ \frac{\partial Z_k}{\partial k} &= \frac{1}{\sqrt{4\pi}}\exp\left(-\frac{U_k''}{Z_k k^2}\right)\left(-\frac{Z_k''}{k^2 Z_k}+\frac{7}{8}\frac{(Z_k')^2}{k^2 Z_k^2}+\frac{3}{2}\frac{Z_k' U_k'''}{k^4 Z_k^2}-\frac{1}{6}\frac{(U_k''')^2}{k^6 Z_k^2}\right).\end{aligned} \tag{20}$$

The algebra including the integral over s is again easily performed by a computer. The result above agrees exactly with the formulae given in [15].

3. Applications and discussion of results

The renormalization group equations obtained in the previous section represent (coupled) nonlinear partial differential equations, which must be solved subject to the appropriate initial condition. Analytic solutions of these equations seem out of the question, and good numerical solutions can also be difficult to calculate. The partial differential equations may be converted into a set of coupled ordinary differential equations, which are then solved on a computer numerically. However, there are various ways of doing this. We will investigate two different methods in this paper. The first method is a Taylor expansion of $U_k(\phi_0)$ and $Z_k(\phi_0)$ about $\phi_0 = 0$,

$$U_k(\phi_0) = \sum_{n=0}^{N}\frac{u_{k,n}}{n!}\phi_0^n, \qquad Z_k(\phi_0) = \sum_{n=0}^{N}\frac{z_{k,n}}{n!}\phi_0^n. \tag{21}$$

If we insert this expansion into the various renormalization group equations developed in the previous section, we obtain a coupled set of $2(N+1)$ ordinary differential equations for the Taylor coefficients $u_{k,n}$ and $z_{k,n}$. Convergence in N must be checked carefully. In practice, it is necessary to use a program for symbolic computation in order to set up the set of differential equations.

We will call our second method the 'method of lines'. Here we discretize $U_k(\phi_0)$ and $U_k''(\phi_0)$ on a suitable N point grid with discretization order M for the derivatives with respect to ϕ_0. For a coupled system $Z_k(\phi_0)$ and its derivatives will be discretized analogously. For example, for $M = 2$ on a homogeneous grid with spacing $\Delta\phi_0$ we use

$$U_{k,i}'' = \frac{U_{k,i+1} - 2U_{k,i} + U_{k,i-1}}{(\Delta\phi_0)^2}. \tag{22}$$

Analogous formulae may be obtained for higher order discretizations as well as for edge points. In this way, one obtains a set of $2N$ coupled ordinary differential equations in the variable k, which is then solved by standard methods such as the (implicit) Runge–Kutta or other methods. In practice, we use the general purpose routines implemented in *Mathematica* to solve the set of ordinary differential equations. For details see the extensive documentation available with this package [19]. It should be pointed out that the routines implemented in this

Table 1. Ground state energy E_0 and energy of first excited state E_1 of the quartic oscillator potential for various couplings g ($N = 30$, $\Lambda = 10^6$, $R_k = k^2$ for SM) calculated from the effective potential. The superscripts SM, WH and PT label the smooth cut-off (equation (8)), the sharp cut-off (equation (9)) and the proper time (equation (10)) version of renormalization flow equation, respectively. The superscript ex labels the result calculated using standard operator quantum mechanics ([20]).

g	E_0^{SM}	E_0^{WH}	E_0^{PT}	E_0^{ex}	E_1^{SM}	E_1^{WH}	E_1^{PT}	E_1^{ex}
0.1	0.5589	0.5586	0.5593	0.5591	1.7696	1.7678	1.7721	1.7695
0.2	0.6019	0.6013	0.6028	0.6024	1.9507	1.9475	1.9556	1.9505
0.3	0.6374	0.6364	0.6386	0.6380	2.0950	2.0906	2.1016	2.0946
0.4	0.6680	0.6667	0.6696	0.6688	2.2174	2.2120	2.2255	2.2169
0.5	0.6953	0.6938	0.6971	0.6962	2.3250	2.3188	2.3343	2.3244
0.6	0.7200	0.7183	0.7221	0.7210	2.4217	2.4148	2.4321	2.4210
0.7	0.7428	0.7409	0.7451	0.7439	2.5100	2.5025	2.5214	2.5092
0.8	0.7639	0.7619	0.7651	0.7651	2.5916	2.5835	2.6038	2.5907
0.9	0.7837	0.7815	0.7864	0.7850	2.6676	2.6590	2.6806	2.6666
1.0	0.8024	0.8000	0.8052	0.8038	2.7389	2.7298	2.7527	2.7379
10.0	1.5009	1.4939	1.5092	1.5050	5.3250	5.3010	5.3617	5.3216
50.0	2.4923	2.4796	2.5068	2.4997	8.9214	8.8787	8.9855	8.9151
100.0	3.1219	3.1057	3.1401	3.1314	11.1952	11.1414	11.2758	11.1873
500.0	5.3032	5.2755	5.3325	5.3199	19.0567	18.9645	19.1901	19.0434
1000.0	6.6730	6.6381	6.7081	6.6942	23.9885	23.8727	24.1525	23.9722

package entail a sophisticated adaptive step-size control mechanism, i.e. the renormalization group equations are solved on a k-grid which is adapted to the problem under consideration.

The specific observables that we will analyse are the ground state energy E_0 (vacuum energy) and the energy gap ΔE_{10}. In terms of the effective potential they are given by

$$E_0 = U_0(\phi_{0,\min}), \qquad \Delta E_{10} = \sqrt{U_0''(\phi_{0,\min})/Z_0(\phi_{0,\min})}, \tag{23}$$

where $\phi_{0,\min}$ denotes the location of the minimum of $U_0(\phi_0)$. Since $U_0(\phi_0)$ is convex, the minimum is uniquely defined.

3.1. Anharmonic oscillator

Before studying systems with tunnelling, we first consider anharmonic oscillators. This will provide insight into the quality of the numerical procedures. The potential, which determines the initial condition, is given by

$$V(x) = \tfrac{1}{2}x^2 + gx^4. \tag{24}$$

The mass and frequency of the oscillator are set to 1 for convenience.

Of the two numerical methods considered here the Taylor expansion described above is numerically the most efficient one, and it produces good results in a relatively short amount of computer time. We investigated expansions up to order $N = 30$ and found good convergence even for large coupling constants g. Results are presented in table 1. They are calculated for $N = 30$ and $\Lambda = 10^6$. For $g < 2$, $N = 20$ is sufficient for convergence. The agreement with calculations using high precision conventional methods [20] is excellent (better than 0.4% even at larger values of g). The numerical values for the ground state energy E_0 calculated using a soft cut-off are systematically somewhat below the conventional calculations. A similar trend is observed for the Wegner–Houghton equation. The PTRG results are systematically slightly above the results obtained with conventional methods, which are believed to be precise to up to six significant figures. The energy gap obtained from the soft cut-off calculations

Table 2. Ground state energy E_0 and energy gap ΔE_{10} for the quartic oscillator potential for various couplings g ($N = 30$, $\Lambda = 10^6$) calculated using equation (17). The superscript ex labels results obtained from standard operator quantum mechanics ([20]). In the last column shows the wavefunction renormalization $Z_0(0)$.

g	E_0^{SM}	E_0^{ex}	$\Delta E_{10}^{\mathrm{SM}}$	$\Delta E_{10}^{\mathrm{ex}}$	$Z_0(0)$
0.1	0.5594	0.5591	1.2107	1.2103	1.0029
0.2	0.6030	0.6024	1.3485	1.3481	1.0052
0.3	0.6389	0.6380	1.4570	1.4567	1.0068
0.4	0.6698	0.6688	1.5485	1.5482	1.0080
0.5	0.6975	0.6962	1.6285	1.6282	1.0088
0.6	0.7225	0.7210	1.7002	1.7000	1.0096
0.7	0.7455	0.7451	1.7655	1.7653	1.0102
0.8	0.7669	0.7651	1.8257	1.8256	1.0107
0.9	0.7869	0.7850	1.8817	1.8816	1.0111
1.0	0.8058	0.8038	1.9341	1.9341	1.0115
10.0	1.5110	1.5050	3.8146	3.8166	1.0167
50.0	2.5105	2.4997	6.4108	6.4153	1.0177
100.0	3.1452	3.1314	8.0498	8.0559	1.0180
500.0	5.3435	5.3199	13.7123	13.7235	1.0183
1000.0	6.7239	6.6942	17.2634	17.2780	1.0184

is systematically slightly above the conventional results and for the hard cut-off and PTRG calculations systematically slightly below them. Generally speaking, the performance of the various renormalization flow equations is very good and leaves little room for improvement. Surprisingly, the numbers obtained using the PTRG equation, which has not been derived rigorously, seem to compare the best with the conventional calculations.

We now include the wavefunction renormalization in our calculations. Here we concentrate on the soft cut-off flow equation (17). Results are shown in table 2. In fact, the analytical expressions for the flow equations of the Taylor coefficients are rather formidable and certainly can only be handled using a computer. However, it appears that a slight improvement on the results without wavefunction renormalization can be achieved. This is particularly noticeable in the calculation for the energy gap, where we now find agreement with conventional calculations to better than 0.03% for coupling constants $g < 2$ and slightly worse for larger g. The calculation of the ground state energy is complicated by the fact that here the large constant Λ enters the calculation and the renormalization flow encompasses several orders of magnitude in the variable k. In general, we find that we achieve worse accuracy for E_0 than for the energy gap. Interestingly, with the wavefunction renormalization Z_k we find ground state energies E_1 that are systematically above the numbers from conventional calculations. The wavefunction renormalization $Z_0(0)$ increases slowly from $Z = 1$ at $g = 0$ to $Z = 1.02$ at $g = 1000$.

Results related to those presented above have been partly obtained before using the Wegner–Houghton equation [8–10] and PTRG equation [15]. The soft cut-off flow equation, which to our knowledge has not been used before in the present context, allows a choice of cut-off functions. We experimented with various power laws and found that the k^2 cut-off function is numerically preferable. However, other power-law cut-off functions may be used if care is taken when choosing the starting point Λ for the evolution.

Once a suitable computer program for solving the renormalization group equations is set up, it is easy to solve other problems as well. We will briefly discuss the sextic oscillator here. Its potential is given by

$$V(x) = \tfrac{1}{2}x^2 + gx^6. \tag{25}$$

Table 3. Ground state energy E_0 and excited state E_1 for the sextic oscillator potential for various couplings g ($N = 24, \Lambda = 10^6$) calculated using equation (17). The superscript ex labels results obtained from standard operator quantum mechanics ([21]). The last column shows the wavefunction renormalization $Z_0(0)$. In the columns with the additional label $Z = 1$ the wavefunction renormalization is not included.

g	$E_0^{\mathrm{SM}}(Z=1)$	E_0^{SM}	E_0^{ex}	$E_1^{\mathrm{SM}}(Z=1)$	E_1^{SM}	E_1^{ex}	$Z_0(0)$
0.01	0.5152	0.5156	0.5154	1.5950	1.5961	1.5954	1.0021
0.1	0.5856	0.5887	0.5869	1.9494	1.9534	1.9505	1.0133
1	0.8006	0.8108	0.8048	2.8734	2.8794	2.8749	1.0270
10	1.2722	1.2950	1.2820	4.7533	4.7610	4.7566	1.0342
100	2.1725	2.2174	2.1925	8.2432	8.2545	8.2542	1.0369

Ground and excited state energies are shown in table 3 and compared to standard calculations [21]. The general trends are similar to those seen for the quartic oscillator. However, it appears that here the wavefunction renormalization becomes more important as is indicated by a more rapidly rising $Z_0(0)$. This indicates that for very steeply rising potentials a local (effective) potential approximation for the effective average action is not sufficient.

3.2. Symmetric double-well potential

We next consider the double-well potential

$$V(x) = -\frac{1}{2}x^2 + gx^4 + \frac{1}{16g}. \tag{26}$$

This is a Z_2 symmetric potential with minima $V(x_m) = 0$ at $x_m = \pm 1/(2\sqrt{g})$ and a barrier between the two wells with height $h = 1/(16g)$. The distance between the minima is given by $d = 1/\sqrt{g}$. For small g the barrier is large and we expect tunnelling to play an important role.

The essential difference between this case and the anharmonic oscillators discussed in the previous section is that the renormalization flow starts from a non-convex classical potential at $k = \Lambda$ and must end at a convex effective potential when $k = 0$. More specifically, the flow of $U_k''(\phi_0)$ starts from $U_\Lambda''(\phi_0) = -1 + 12g\phi_0^2$, which is negative between $-x_m/\sqrt{3}$ and $+x_m/\sqrt{3}$, and must end with $U_0''(\phi_0) > 0$. During the flow $U_k''(\phi_0)$ must fulfil the relation $U_k''(\phi_0) > -k^2$ for the soft and hard cut-off RG equations, otherwise the renormalization flow would become singular at some point during the flow. Such a stringent condition does not hold for the PTRG, which simplifies the numerical solution significantly.

Let us illustrate the features described above with numerical examples obtained using the method of lines for relatively small couplings $g = 0.05$ and $g = 0.01$: as can be seen in figure 1, the effective potential for $k = 0$ is nearly flat between the two wells. Close to the minima the effective potential bends up sharply to a steep rise. At about the minima of the classical potential the effective potential bends towards the classical potential and follows it for large $|\phi_0|$. These features are expected from a qualitative analysis of the RGEs. The crossing of the effective potential with the y-axis marks the value of the ground state energy. Obviously, it is already deeply below the top of the barrier.

It is interesting to study the behaviour of the flow of $U_k''(\phi_0)$ close to $k = 0$, since it drives the partial differential equation (8). This is shown in figure 2. Obviously, $U_k''(\phi_0)$ stays at its initial value until it bends towards the line $-k^2$ at around $k \sim 1$. For very small couplings g, we see a rather complicated structure for $k < 1$. In particular, for ϕ_0 between the classical minima, the flow follows the line $-k^2$ rather closely at small k. Therefore, in this range of

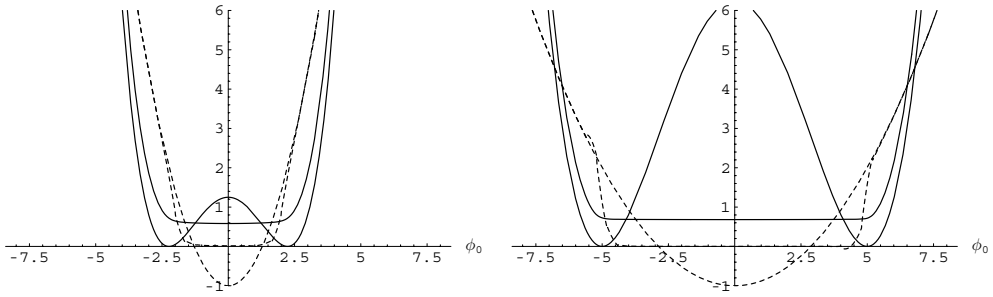

Figure 1. Effective potential and its second derivative calculated from the soft cut-off RGE for $g = 0.05$ (left) and $g = 0.01$ (right) ($\Lambda = 1500$). Full lines: $U_0(\phi_0)$ at the beginning (double well) and at the end of the flow (convex). Short-dashed lines: $U_0''(\phi_0)$ at the beginning and the end of the flow. The calculations were done on grid with 100 points evenly distributed between $\phi_0 = -20$ and $\phi_0 = -20$ using the method of lines. Discretization order $M = 3$.

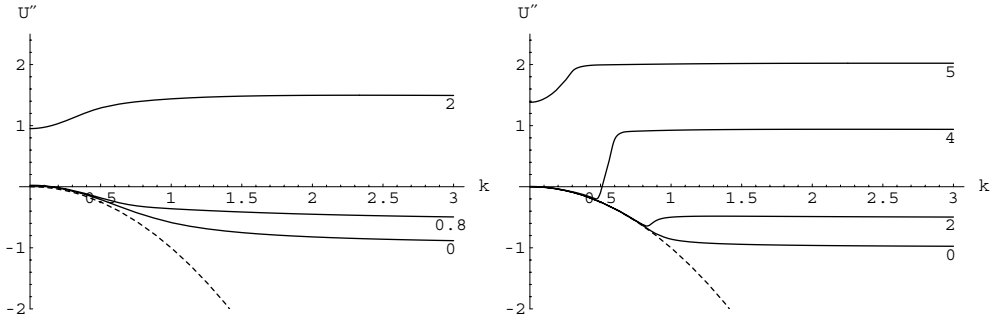

Figure 2. Flow of $U_k''(\phi_0)$ versus k calculated using the soft cut-off RGE for $g = 0.05$ and $\phi_0 = 0, 0.8, 2$ (left) and $g = 0.01$ and $\phi_0 = 0, 2, 4, 5$ (right) ($\Lambda = 1500$). The short-dashed line represents $-k^2$. The flow of $U_k''(\phi_0)$ never crosses the line $-k^2$, but follows it closely for small k and ϕ_0.

parameters the flow may be described by the formula $U_k''(\phi_0) = a - k^2$ with $0 < a \ll 1$ for small g. For ϕ_0 beyond the minima of the wells the flow remains very close to its initial value.

Unfortunately, already for the uncoupled equation (8) it proves to be rather difficult to obtain the structure just described with sufficient accuracy in a numerical analysis. There are two obstacles: firstly, the numerical procedure must be accurate enough that it does not hit the line $-k^2$ accidentally due to numerical inaccuracies. This is difficult for small g, since the difference between $-k^2$ and $U_k''(\phi_0)$ is extremely small. Secondly, if one increases the spacial resolution of the numerical grid in an attempt to describe this structure more precisely, one runs into instabilities due to discretization errors. In practice, it is necessary to chose the spacing of the discretization grid and the discretization order M carefully in order to steer the calculation clear of the problems just described. Similar considerations hold for the hard cut-off Wegner–Houghton equation, since it shows the same singularity as the soft cut-off equation.

We now consider the equations with wavefunction renormalization, equation (17). Similar considerations hold for equation (18). Here, the singularity discussed above appears in each term of the equation for Z_k. We observe that coupling between the two equations for $U_k(\phi_0)$ and $Z_k(\phi_0)$ only occurs through the last term $\sim Z_k(U_k''')^2$ in the equation for $Z_k(\phi_0)$. If this term is absent, one easily shows that $Z_k(\phi_0) = 1$ solves the coupled equations. So the

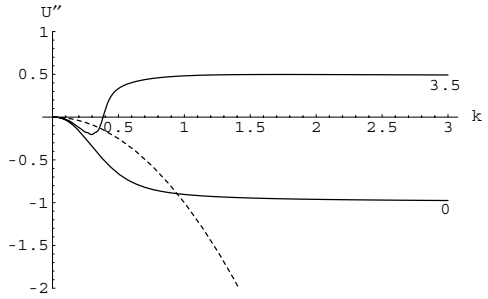

Figure 3. Flow of $U_k''(0)$ calculated using the PTRG for $g = 0.01$ and $\phi_0 = 0, 3.5$ ($\Lambda = 1500$). The short-dashed line represents $-k^2$. Here the flow crosses the line $-k^2$.

behaviour of $U_k'''(\phi_0)$ is critical for a practical solution of the coupled equations. From our considerations above we know that the effective potential closely follows the classical potential for ϕ_0 somewhat beyond the minima of the classical potential. Consequently, in this parameter range $U_k'''(\phi_0) = 0$ and $Z_k(\phi_0) = 1$. It is in the region around the minima of the potential that $U_k'''(\phi_0)$ is markedly different from zero and, therefore, $Z_k(\phi_0) \neq 1$.

However, it is the critical term $\sim(U_k''')^2$, which increases numerical instabilities: firstly, numerical uncertainties in the determination of U_k''' enter quadratically. Secondly, the small term $k^2 + U_k''$ enters with an inverse cubic power. As a result, the essential driving term for the evolution of Z_k cannot be determined with sufficient numerical accuracy and the evolution of Z_k becomes unstable even for coupling constants around $g = 0.1$, where $Z_0(0)$ is expected to be significantly different from 1.

For the PTRG the situation is different, since the PTRG does not enforce the condition $U_k''(\phi_0) > -k^2$. An example is shown in figure 3. The line $-k^2$ is crossed by the flow. This different flow pattern simplifies the practical solution of the PTRG significantly. For $k \ll 0.1$ the flow develops the form $U_k''(\phi_0) \sim a - bk^2$ with constants $a > 0, b > 0$. Also in the case of the PTRG , it is the term $U_k'''(\phi_0)$ which couples equations (20) for U_k and Z_k. These coupled equations are much easier to solve numerically than equation (8) or (9), since the equations do not require $U_k''(\phi_0) > -k^2$.

From the discussion above, it appears that highly accurate calculations require a numerical method which specifically takes into account the singular structure of the RGE. In this paper, however, we will limit the discussion to results obtained using general purpose solvers for the set of nonlinear differential equations. Such techniques are limited, and we will explore the limitations in the following discussion. A Taylor expansion technique will not be able to describe the flow pattern, which develops for small g and ϕ_0 for the soft or hard cut-off RGE. In fact, it runs rather soon into the singularity $U_k''(\phi_0) = -k^2$, and the effective potential cannot be calculated for k below the singular point. However, it works surprisingly well for the PTRG.

At small ϕ_0 the effective potential may be expanded into a Taylor series. As is seen from figure 4 the Taylor expansion technique does manage to produce the nearly flat potential between the two minima correctly. It is the behaviour of the effective potential close to the minima of the classical potential and beyond which cannot be reproduced by this technique as is seen from a comparison with figure 1. For these calculations we used $N = 20$, which is enough for convergence.

We now discuss the spectra obtained quantitatively. We first present the spectra obtained from equations (8), (9) and (10) using the Taylor expansion (21) of the effective potential.

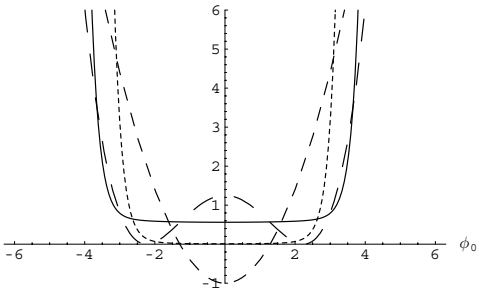

Figure 4. The effective potential for $g = 0.05$ calculated using a Taylor expansion. Long-dashed lines: classical potential. Full line: effective potential $U_0(0)$. Short-dashed line: second derivative of classical potential. Dotted line: second derivative of effective potential ($N = 20$, $\Lambda = 1500$).

Table 4. Ground state energy E_0 and energy of first excited state E_1 of the double-well potential for various couplings g calculated using a Taylor expansion ($N = 20$, $\Lambda = 10^4$). The superscripts SM, WH and PT label the smooth cut-off, the hard cut-off and the proper time version of ERGE, respectively. The superscript ex labels the result calculated with standard operator quantum mechanics ([22–25]).

g	E_0^{SM}	E_0^{WH}	E_0^{PT}	E_0^{ex}	E_1^{SM}	E_1^{WH}	E_1^{PT}	E_1^{ex}
0.05	0.5616	–	0.6192	0.6173	0.6595	–	0.6821	0.6735
0.06	0.5542	0.5405	0.5998	0.5813	0.7149	0.7275	0.7263	0.6844
0.07	0.5247	0.5325	0.5648	0.5469	0.7292	0.8078	0.7485	0.7008
0.08	0.4984	0.4932	0.5322	0.5168	0.7421	0.8035	0.7680	0.7210
0.09	0.4766	0.4636	0.5047	0.4915	0.7599	0.7973	0.7886	0.7436
0.1	0.4585	0.4432	0.4823	0.4709	0.7818	0.8002	0.8105	0.7678
0.5	0.4504	0.4436	0.4576	0.4526	1.5461	1.5269	1.5694	1.5423
1.0	0.5740	0.5678	0.5809	0.5773	2.0865	2.0675	2.1111	2.0831
10.0	1.3730	1.3638	1.3830	1.3778	5.0002	4.9703	5.0418	4.9957
100.0	3.0602	3.0418	3.0792	3.0701	11.0422	10.9807	11.1250	11.0337

It was suggested in [10] that such an approach is not suitable in general. However, we find that down to couplings $g = 0.05$, which were also considered in [10], a Taylor expansion does work at the 10% level or better, as is shown in table 4. Not surprisingly, one finds that the PTRG renormalization group performs better than the other approaches. Here the agreement is better than 4% for the ground state energy and better than 20% for the energy gap. For couplings g smaller than 0.05, all RGE run into a singularity or instability and the ground state energy and the energy gap cannot be determined. This situation does not improve if one includes the wavefunction renormalization.

In the following, we use the method of lines, which takes into account the details of the renormalization flow correctly also at large ϕ_0. The results for the spectrum are presented in table 5 as well as in figures 5.

We observe that the smooth cut-off equation determines the ground state energy in agreement with conventional calculations on the 1% level over the whole range of coupling constants. This is significantly better than the results obtained in [10] using the Wegner–Houghton equation, where the ground state energy was too small for small coupling constants. Indeed, our calculations for the Wegner–Houghton equation also lead to a ground state energy which is too small. The reason for this is still not fully understood, but we attribute it to numerical difficulties. Moreover, for the hard and soft cut-off RGE we are unable to determine the wavefunction renormalization reliably for small g due to numerical difficulties connected

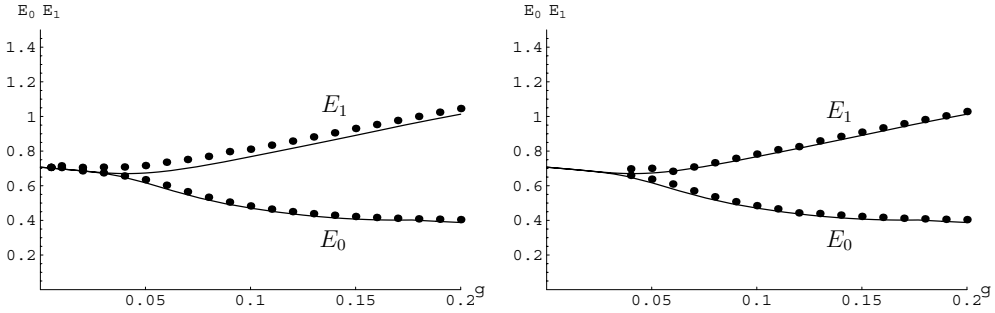

Figure 5. (left) Ground state energy E_0 and excited state energy E_1 calculated with the PTRG equation (10) using the method of lines with 100 points evenly distributed between $\phi_0 = -5$ and $\phi_0 = 5$, discretization order $M = 2$ (dots). Full lines: exact result using conventional methods (right). The same calculation including the wavefunction renormalization, discretization order $M = 2$.

Table 5. Ground state energy E_0 and energy gap ΔE_{10} for the double-well potential calculated using the method of lines ($\Lambda = 1500$). The superscripts SM and PT label the smooth cut-off and the proper time version of ERGE, respectively. The superscript ex labels the result calculated with standard operator quantum mechanics ([22–25]).

g	$E_{0,Z=1}^{\mathrm{SM}}$	$E_{0,Z=1}^{\mathrm{PT}}$	E_0^{PT}	E_0^{ex}	$\Delta E_{10,Z=1}^{\mathrm{SM}}$	$\Delta E_{10,Z=1}^{\mathrm{PT}}$	$\Delta E_{10}^{\mathrm{PT}}$	$\Delta E_{10}^{\mathrm{ex}}$
0.01	0.6942	0.7050	–	0.6968	0.0197	0.0098	–	0.0
0.02	0.6791	0.6870	–	0.6856	0.0447	0.0194	–	0.0001
0.03	0.6451	0.6766	–	0.6715	0.0691	0.0359	–	0.0036
0.04	0.6201	0.6565	0.6796	0.6491	0.0953	0.0517	0.0324	0.0210
0.05	0.5926	0.6347	0.6457	0.6173	0.1273	0.0817	0.0440	0.0562
0.06	0.5640	0.6028	0.6000	0.5813	0.1634	0.1329	0.0739	0.1030
0.07	0.5357	0.5657	0.5711	0.5469	0.1882	0.1859	0.1394	0.1539
0.08	0.5103	0.5335	0.5362	0.5168	0.2464	0.2360	0.1964	0.2041
0.09	0.4882	0.5057	0.5079	0.4915	0.2882	0.2914	0.2500	0.2520
0.10	0.4627	0.4833	0.4850	0.4709	0.3258	0.3276	0.2978	0.2969
0.20	0.3960	0.4045	0.4043	0.3975	0.6321	0.6413	0.6241	0.6159
0.30	0.4046	0.4107	0.4085	0.4043	0.8402	0.8411	0.8252	0.8166
0.40	0.4286	0.4336	0.4319	0.4272	0.9806	0.9864	0.9761	0.9666

with the singularity. The energy gap is obtained in reasonable agreement with conventional calculations. To obtain the extremely small energy gap at small g correctly requires numerical procedures with extremely high accuracy, since the energy gap is obtained from the square root of U_k'', e.g. for $g = 0.3$ we expect $U_k'' < 10^{-5}$.

The ground state energy determined from the PTRG equation is slightly too large for small g when compared to conventional calculations. For the energy gap we essentially confirm the results presented in [15]. The wavefunction renormalization definitely improves the calculation of the energy gap, while it does not improve the calculation of the ground state energy. This feature remains to be clarified.

3.3. Supersymmetric model

The 0D supersymmetric model proposed by Witten [26], which is described by the Hamiltonian

$$H = \frac{1}{2}\left(p^2 + w^2(x) + \sigma_3 \frac{\mathrm{d}w(x)}{\mathrm{d}x}\right) \tag{27}$$

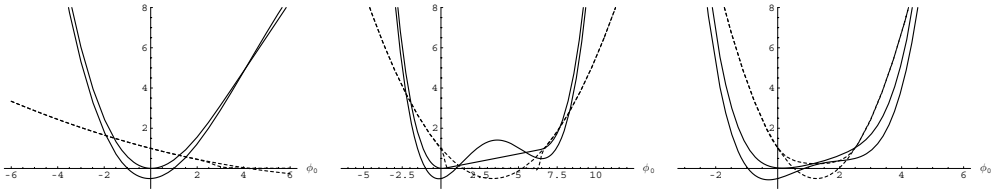

Figure 6. Effective potential and its second derivative calculated from the soft cut-off RGE for $g = 0.05$ (left), $g = 0.15$ (centre) and $g = 0.4$ ($\Lambda = 1500$). Full lines: $U_0(\phi_0)$ at the beginning of the flow (double well) and at the end of the flow (convex). Short-dashed lines: $U_0''(\phi_0)$ at the beginning and at the end of the flow. The calculations are done on grid with 120 points evenly distributed between $\phi_0 = -10$ and $\phi_0 = 15$ using the method of lines. Discretization order $M = 3$.

shows dynamical breaking of supersymmetry, i.e. the Hamiltonian commutes with the operators $Q_1 = \frac{1}{2}(\sigma_1 p + \sigma_2 w(x))$ and $Q_2 = \frac{1}{2}(\sigma_2 p - \sigma_1 w(x))$, but the ground state is not an eigenstate of these operators. The σ_i are Pauli matrices, p is the momentum operator and $w(x) = gx^2 - x$ with g a parameter.

Here we would like to study the spectrum of this model quantitatively. This has been done before in [8] using the Wegner–Houghton equation. The Hamiltonian above may be diagonalized in Pauli space

$$H = \begin{pmatrix} \frac{1}{2}p^2 + V_+(x) & 0 \\ 0 & \frac{1}{2}p^2 + V_-(x) \end{pmatrix} \tag{28}$$

with $V_\pm = \frac{1}{2}(w^2(x) \pm \mathrm{d}w(x)/\mathrm{d}x)$. Consequently, we are led to investigate the potential

$$V_+(x) = \tfrac{1}{2}g^2x^4 - gx^3 + \tfrac{1}{2}x^2 + gx - \tfrac{1}{2}. \tag{29}$$

The potential $V_+(x)$ is an asymmetric double well for $0 < g < 0.31$ and a single well for $g > 0.31$. The barrier between the wells is small close to $g \sim 0.31$, and increases for $g \to 0$. However, since the well is asymmetric, the spectrum differs qualitatively from that of the Z_2 symmetric double-well studied in the previous section. This is shown in figure 6. The minimum of the classical potential is found somewhat below $\phi_0 = 0$, and the effective potential $U_0(\phi_0)$ shows its (positive) minimum slightly above $\phi_0 = 0$. The value of $U_0(\phi_0)$ at the minimum determines the ground state energy. Close to this point $U_0''(\phi_0)$ drops to zero for $g < 0.31$, and we obtain $U_0''(\phi_{0,\min})$ somewhere between 0.5 and 1. It is the structure of the effective potential close to the minimum of the classical potential which determines the spectrum, unlike in the case of the symmetric double well, where the structure between the two wells determines the spectrum. As we have seen in the previous subsection, the Taylor expansion technique used in [8] is not able to describe the effective potential in the region around the classical minima. This is the reason why the results obtained in [8] are unsatisfactory.

It can be shown that the dynamical breaking of supersymmetry shown by the model equation (28) is related to a non-vanishing ground state energy. Perturbation theory predicts a ground state energy $E_0 = 0$ for the potential V_+, so the dynamical breaking of supersymmtry is clearly a non-perturbative effect, which is easily obtained by the techniques employed here. The calculated spectrum is shown in figure 7. The calculation shown in the left plot has been done with the soft cut-off RG equation (8) using the method of lines. Obviously the ground state energy is obtained in agreement with conventional calculations, but E_1 is somewhat too large. If we include the wavefunction renormalization using equation (8) the agreement with conventional calculations clearly improves as shown on the right plot in figure 7. However,

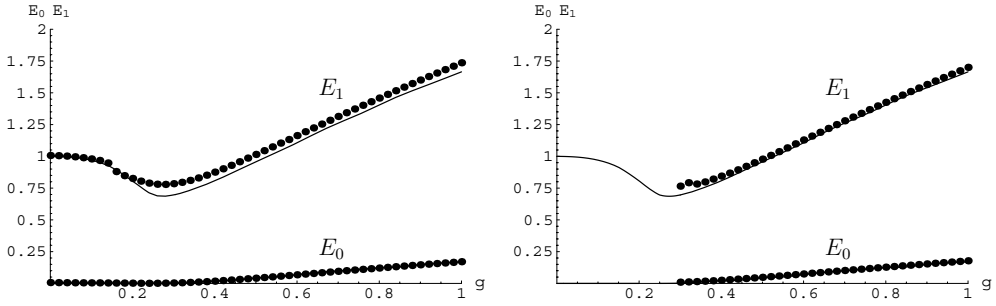

Figure 7. (left) Ground state energy E_0 and excited state energy E_1 calculated with the soft cut-off RG equation (8) using the method of lines with 100 points evenly distributed between $\phi_0 = -10$ and $\phi_0 = 8$, discretization order $M = 3$ (dots). Full lines: exact result using conventional methods (right). The same calculation including the wavefunction renormalization.

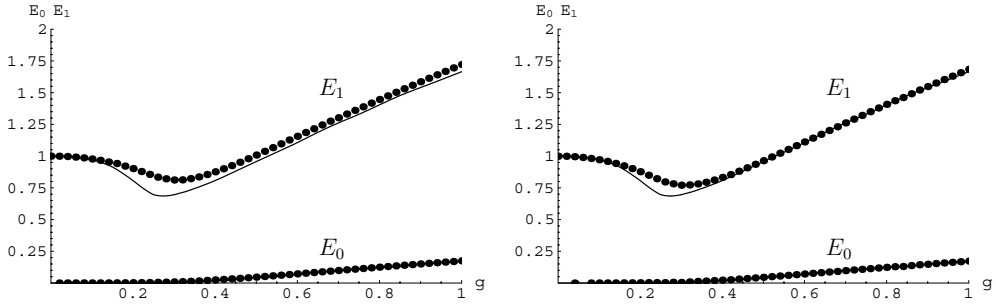

Figure 8. (left) Ground state energy E_0 and excited state energy E_1 calculated with the PTRG equation (10) using the method of lines with 90 points evenly distributed between $\phi_0 = -4$ and $\phi_0 = 7$, discretization order $M = 3$ (dots). Full lines: exact result using conventional methods (right). The same calculation including the wavefunction renormalization, discretization order $M = 2$.

with the numerical methods presently employed we are unable to solve the coupled equations correctly in the parameter region $g < 0.3$.

Using the PTRG equation (10) we obtain similar results as shown in figure 8. The numerical calculation is significantly faster than in the case of the soft cut-off RGE, since there is no singularity which needs to be avoided during the renormalization flow. This problem has been discussed in detail in the previous section. Again, consideration of the wavefunction renormalization via equation (20) improves agreement with conventional calculations. Obviously, there is still some disagreement with conventional calculations in the parameter range, where E_1 shows a minimum. The reason for this discrepancy is presently not clear.

4. Conclusions

Previous work [15] using the Schwinger time renormalization group equation (PTRG) suggests that consideration of the wavefunction renormalization improves the description of quantum systems influenced by tunnelling processes. Since the PTRG cannot be rigorously derived, in the present paper we undertake an analogous investigation on the basis of the soft cut-off renormalization group equations derived by Wetterich and Morris as well as the hard cut-off

equation originally proposed by Wegner and Houghton. To this end we derive a partial differential equation for the wavefunction renormalization $Z_k(\phi_0)$, which supplements the well-known equation for the effective potential $U_k(\phi_0)$. The derivation is based on a standard gradient expansion of the effective average action. It is found that the soft cut-off clearly performs quantitatively better than the hard cut-off procedure, which is preferred by some investigators (see e.g. [11]).

We then analyse the resulting set of coupled partial differential equations qualitatively and numerically. It is shown that the solutions for the soft and hard cut-off equations differ qualitatively from those of the PTRG at small k. This is essentially due to the fact that the soft and hard cut-off equations must fulfil the relation $U_k''(\phi_0) > -k^2$ during the renormalization flow, in order to avoid a singularity of the flow equations. This condition proves to be a numerical difficulty in those parameter ranges where tunnelling is important.

Using the renormalization group equations we calculate the spectra for four examples, a quartic anharmonic oscillator, a sextic anharmonic oscillator, a symmetric and an asymmetric double well. The spectra obtained agree well with results from conventional calculations, in particular, if the wavefunction renormalization is included. However, for the soft and hard cut-off renormalization group equations, we are presently unable to solve the coupled partial differential equations for the wavefunction renormalization Z_k with sufficient accuracy in the region where tunnelling plays an important role. This is due to the singularity mentioned above. In the case of the PTRG the equations can be solved easily, and good numerical results are achieved.

Finally, it is interesting to note that in every respect investigated here the PTRG equation performs better than the soft and hard cut-off equations. Its only disadvantage seems to be that a rigorous derivation of this equation is not known.

Acknowledgments

I would like to acknowledge the help of Janusz Szwabinski, who participated in the early stages of this work. Furthermore, I would like to thank Marcel Reginatto for a careful reading of the paper.

Appendix. Some useful formulae from operator algebra

Here we briefly review a few operator identities, which we need for our calculations.

Let A and B operators. The Hadamard formula is given by

$$\mathrm{e}^{tB} A \, \mathrm{e}^{-tB} = A + t[B, A] + \frac{t^2}{2!}[B, [B, A]] + \cdots . \tag{A.1}$$

We use this formula in order to prove the relation

$$A\frac{1}{B} = \frac{1}{B}A + \frac{1}{B^2}[B, A] + \frac{1}{B^3}[B, [B, A]] + \cdots . \tag{A.2}$$

This result enables us to move the innermost $1/B$ operator in equation (15) to the left. Setting $A = A_1$ one obtains

$$Q(\tau) = \mathrm{e}^{-\mathrm{i}\tau\omega}\left(\frac{1}{B} - \frac{1}{B}A_1\frac{1}{B} + \frac{1}{B^2}A_1^2\frac{1}{B} + \frac{1}{B^3}[B, A_1]A_1\frac{1}{B} + \frac{1}{B^4}[B, [B, A_1]]A_1\frac{1}{B}\right)\mathrm{e}^{\mathrm{i}\tau\omega} + \cdots . \tag{A.3}$$

In order to derive the derivative expansion for the PTRG renormalization group equation we need the Zassenhaus formula [18, 27], which is given by

$$\mathrm{e}^{A+B} = \mathrm{e}^{A}\,\mathrm{e}^{B}\prod_{i=2}^{\infty}\mathrm{e}^{C_i}, \tag{A.4}$$

where

$$\begin{aligned} C_2 &= \tfrac{1}{2}[B, A], \\ C_3 &= \tfrac{1}{3}[[B, A], B] + \tfrac{1}{6}[[B, A], A], \\ C_4 &= \tfrac{1}{8}[[[B, A], B], B] + \tfrac{1}{8}[[[B, A], A], B] + \tfrac{1}{24}[[[B, A], A], A]. \end{aligned} \tag{A.5}$$

This formula allows one to disentangle two exponentials.

Setting $A = -sA_0$ and $B = -sA_1$ one obtains

$$\mathrm{e}^{-s(A_0+A_1)} = \mathrm{e}^{-sA_0}\,\mathrm{e}^{-sA_1}\,\mathrm{e}^{C_2}\,\mathrm{e}^{C_3}\,\mathrm{e}^{C_4}\cdots. \tag{A.6}$$

We now expand this product of exponential operators up to $O(s^4)$ and obtain

$$\begin{aligned} \mathrm{e}^{-s(A_0+A_1)} = \mathrm{e}^{-sA_0}\Big\{ & 1 - sA_1 + \frac{s^2}{2}\big(A_1^2 + [A_1, A_0]\big) \\ & - \frac{s^3}{6}\big(A_1^3 + 3A_1[A_1, A_0] + 2[[A_1, A_0], A_1] + [[A_1, A_0], A_0]\big) \\ & + \frac{s^4}{24}\big(A_1^4 + 6A_1^2[A_1, A_0] + 3[A_1, A_0]^2 + 8A_1[[A_1, A_0], A_1] \\ & + 4A_1[[A_1, A_0], A_0] + 3[[[A_1, A_0], A_1], A_1] \\ & + 3[[[A_1, A_0], A_0], A_1]) + [[[A_1, A_0], A_0], A_0]\big)\Big\}. \end{aligned} \tag{A.7}$$

Terms with more than two A_1 operators do not contribute to the equation for Z_k. We also explicitly checked that terms in higher than fourth order in s do not contribute to the equation for Z_k.

References

[1] Langer J S 1967 *Ann. Phys.* **41** 108
[2] Wilson K G and Kogut I G 1974 *Phys. Rep.* **12** 75
[3] Wegner F J and Houghton A 1973 *Phys. Rev.* A **8** 401
[4] Polchinski J 1984 *Nucl. Phys.* B **231** 269
[5] Wetterich C 1993 *Phys. Lett.* B **301** 90
[6] Morris T R 1994 *Int. J. Mod. Phys.* A **9** 2411
[7] Bagnuls C and Bervillier C 2001 *Phys. Rep.* **348** 91–157
[8] Aoki K, Horikoshi A, Taniguchi M and Terao H 1999 *Proc. of the Workshop on the Exact Renormalization Group (Faro, Portugal, Sept. 1998)* (*Preprint* hep-th/9812050)
[9] Gosselin P, Grosdidier B and Mohrbach H 1999 *Phys. Lett.* A **256** 125–31
[10] Kapoyannis A S and Tetradis N 2000 *Phys. Lett.* A **276** 225–32
[11] Hedden R, Meden V, Pruschke T and Schönhammer K 2004 *J. Phys.: Condens. Matter* **16** 5279–96
[12] Weyrauch M Functional renormalization group: truncation schemes and quantum tunnelling *J. Mol. Liq.* submitted
[13] Berges J, Tetradis N and Wetterich C 2002 *Phys. Rep.* **363** 223–386
[14] Bonanno A and Zappalà D 2001 *Phys. Lett.* B **504** 181
[15] Zappala D 2001 *Phys. Lett.* A **290** 35–40
[16] Hasenfratz A and Hasenfratz P 1986 *Nucl. Phys.* B **270** 687
[17] Bonanno A and Zappala D 1998 *Phys. Rev.* D **57** 7383
[18] Magnus W 1954 *Commun. Pure Appl. Math.* **7** 649–73

[19] Wolfram S 2004 *The Mathematica Book* 5th edn (Champaign, IL: Wolfram Media)
[20] Hioe F T, MacMillen D and Montroll E W 1978 *Phys. Rep.* **43** 305–35
[21] Castellani C, Di Castro C, Pistolesi F and Strinati G C 1997 *Phys. Rev. Lett.* **78** 1612
[22] Banerjee K and Bhatnagar S P 1978 *Phys. Rev.* D **18** 4767
[23] Balsa R, Plo M, Esteve J G and Pacheco A F 1983 *Phys. Rev.* D **28** 1945
[24] Hsue C S and Chern J L 1984 *Phys. Rev.* D **29** 643–647
[25] Zhou F, Cao Z and Shen Q 2003 *Phys. Rev.* A **67** 062112
[26] Witten E 1981 *Nucl. Phys.* B **188** 513
[27] Scholz D and Weyrauch M A note on the Zassenhaus product formula *J. Math. Phys.* submitted